A Constitutive Model for Elastic Damage in Fiber-Reinforced PMC Laminae

EVER J. BARBERO[1] AND LILIANA DE VIVO
West Virginia University
Morgantown, WV 26506-6106

ABSTRACT: A practical methodology is presented for modeling the damaging behavior of fiber-reinforced, polymer-matrix composite laminae. It accounts for the basic mechanisms of degradation of properties under mechanical loading and incorporates this knowledge into a simple constitutive model in the framework of Continuum Damage Mechanics. A new expression for the damage surface is proposed, which reduces to the expression of the Tsai-Wu failure criterion in stress space. Model identification allows us to characterize the material through a small number of material parameters, all of which are related to material properties available in the literature. Available experimental results are used to illustrate the proposed methodology.

KEY WORDS: PMC, FRP, composite, damage, parameter identification, failure, critical damage.

1. INTRODUCTION

POLYMER MATRIX COMPOSITE (PMC) are widely used because of their high strength to weight ratio, resistance to environmental deterioration, lack of interference with electromagnetic radiation and so on. Because of the manufacturing-induced defects, composites cannot be considered defect free in their virgin unloaded state. It has been observed that micro-defects and micro-cracks can grow to a potentially critical size, even in the case of monotonic loading conditions. In order to fully exploit the potential of composites, it is therefore necessary to model the development of damage. Micro-mechanical and material science based models have been developed and applied in order to explore the circumstances related to the damage of either the fibers or the matrix separately [15,24]. Micromechanics can be used to assemble global response of the material [25–27]. The most significant limitation of those models resides in the large number of material parameters

[1]Author to whom correspondence should be addressed.

1056-7895/01/01 0073–21 $10.00/0 DOI: 10.1106/6PQ6-31JW-F69K-74LU

needed to identify the constitutive model and the high computational effort involved.

In order to conjugate simplicity of application and accuracy of results, the concept of distributed damage and the use of formulations based on the thermodynamics of continuum media plays a fundamental role. In this framework, Continuum Damage Mechanics (CDM) considers damaged materials as a continuum, in spite of heterogeneity, micro-cavities, and micro-defects. The response to the loading conditions is determined on the basis of the constitutive relations between macroscopic variables (e.g., stress, strain) and internal variables which model, on a macroscopic scale, the irreversible changes occurring at the microscopic level.

Therefore, the objective of this paper is the definition, in the framework of CDM, of a constitutive model for a single lamina of fiber-reinforced PMC in order to predict the nonlinear behavior due to damage phenomena. At the elementary ply scale, the fiber-reinforced composite is considered as an ideal homogeneous and transversely isotropic material. The model is identified by means of a finite number of material parameters, which can be easily determined and are characteristic of the material. Furthermore, the parameter identification is done entirely in terms of available experimental data without need of additional testing.

2. THE DAMAGE TENSOR

Damage phenomena in the matrix consist of cracking, which occurs under tensile loading when the strength of the matrix is exceeded. Two stages can be identified. The first stage consists of the initiation and growth of multiple cracking of the matrix in the direction normal to the load. However, cracks are confined to the matrix alone and increase only in number; the average size of cracks is smaller than the fiber spacing and the damage mode is then characterized as a dispersed matrix damage. In the second stage, some localization at preferred sites takes place. When a crack is long enough to strike the interface with a fiber, further growth may be prevented if the stress at the crack tip is insufficient to break the fiber. If the interfacial fiber-matrix strength is low, a diversion of the crack in the fiber direction can be observed leading to transverse fiber debonding. Matrix cracking is the dominant damage mode when the loading direction is inclined with respect to the fiber direction. The tip of a crack in the matrix is subject to two displacement components: one normal to the fibers and one parallel to them. At an off-axis angle of 90°, the opening component will be coincident with the total displacement and it will induce crack opening in the matrix, leading to transverse fiber debonding.

Different damage mechanisms appear in the fibers depending on the type of stress, compressive or tensile, along the fiber direction. Under tensile stress, the damage is proportional to the number of broken fibers [23]. Since fibers are mostly brittle, a surface crack may grow instantaneously across its cross-section. Therefore, a fiber may break either at the weakest point along its length, or at the point of highest stress concentration.

In compression, the damage mechanism appears to be related to fiber micro-buckling [2,29]. If the fibers buckle symmetrically about one another, a transverse or extensional mode appears, where the matrix alternately deforms in extension and compression transverse to the fibers. However, the most commonly observed is the shear mode, where the fibers buckle in phase with one another so that the matrix is subject to shearing deformations [7]. Each fiber or fiber bundle buckles under different value of local stress depending on the magnitude of the local imperfections, namely fiber misalignment [28].

Composites with brittle matrices and a relatively weak interfacial bond (such as glass or aramid fibers in polyester resins) are characterized by extensive debonding when subject to longitudinal tensile loading [19]. The damage mode is often described as brush-like; by examining the broken specimen, it is impossible to identify the point at which the crack initiated, or its path. On the other hand, when the interface between fibers and matrix is relatively strong, composites fail by propagation of a single crack across its section, with little or no longitudinal debonding. Such a behavior is observed in some carbon/epoxy composites.

A number of theories have been developed to model anisotropic damage states by means of damage variables ranging from vectors to higher order tensors [13]. Since the stress and the material response of composites are both direction dependent, the resulting damage is, in principle, anisotropic [15]. However, the main modes of damage in composites are fiber breaks, fiber-matrix debond, and matrix cracking along and/or perpendicular to the fiber direction. Therefore, damage can be approximated well as orthotropic with orientations coincident with the material directions. Consequently, in this work, the damage of the material is described by means of a second-order tensor **D**, called *damage tensor*. The eigenvalues D_i describe the net area reduction on the three planes orthogonal to the principal direction of the tensor **D**. Similarly, the symmetric tensor $\Omega = \sqrt{I - D}$, whose eigenvalues can be related to the load-carrying area in the same three planes, will be denoted as the *integrity tensor*. Having defined the damage tensor **D**, the effective stress can be computed as

$$\bar{\boldsymbol{\sigma}} = \mathbf{M}^{-1}(\mathbf{D})\boldsymbol{\sigma} \tag{1}$$

where the fourth-order tensor **M** is called *damage effect tensor*. The symmetric effective stress tensor $\bar{\boldsymbol{\sigma}}$ in the effective configuration $\bar{\mathcal{L}}$ may be obtained by pushing back the stress tensor $\boldsymbol{\sigma}$ in the damaged configuration [6,17] according to

$$\bar{\boldsymbol{\sigma}} = (\Omega^{-1} \boxtimes \Omega^{-1})\boldsymbol{\sigma} = [(\sqrt{\mathbf{I} - \mathbf{D}})^{-1} \boxtimes (\sqrt{\mathbf{I} - \mathbf{D}})^{-1}]\boldsymbol{\sigma} \tag{2}$$

where the symbol $\boxtimes$ denotes the product of two second-order tensors defined as

$(\mathbf{A} \boxtimes \mathbf{B})\mathbf{C} = \mathbf{ACB}^T$. By comparing definitions (1) and (2), the doubly-symmetric fourth-order damage effect tensor **M** can be written as

$$\mathbf{M}(\mathbf{D}) = \Omega(\mathbf{D}) \boxtimes \Omega(\mathbf{D}) \quad \text{or} \quad M_{ijkl} = \Omega_{ik}\Omega_{lj} \tag{3}$$

The expression of the doubly-symmetric damaged elastic stiffness **E** follows from the hypothesis of equivalent elastic energy between the damaged configuration $\pounds$ and the effective one $\bar{\pounds}$. Hence, Equation (1) yields

$$\mathbf{E} = \mathbf{M}\bar{\mathbf{E}}\mathbf{M}^T = \mathbf{M}\bar{\mathbf{E}}\mathbf{M} \tag{4}$$

3. THE CONSTITUTIVE MODEL

3.1 Kinematic and Static Variables

Besides the elastic strain $\boldsymbol{\varepsilon}$ belonging to the linear space $\mathcal{D}$, let us assume the second-order symmetric tensor **D** as kinematic internal variable in order to represent the orthotropic state of damage characterized by micro-cracks and micro-defects. The damage tensor belongs to the linear space $\mathcal{X}_1$, which however depends on the limit values D_c of the load-carrying area reduction in the three planes orthogonal to the principal directions of **D**.

In the case of unidirectional fiber-reinforced laminae, preferential directions for damage growth can be determined from a phenomenological point of view. As already pointed out, it may be said that micro-cracks and micro-defects will appear and develop along the direction of the fibers and along the direction orthogonal to them; that is parallel to the material principal direction of the lamina. Therefore, the principal directions of the damage tensor D are assumed to be coincident with the material directions and constant throughout the damage process. They are supposed to be known and do not necessarily coincide with the principal directions of stress. The eigenvalues D_1, D_2 and D_3 are representative of the net area reduction in the three principal material planes, and each of them ranges between 0 and the relevant limit value: $D_i \in [0, D_i^{cr}]$, $i = 1,2,3$.

An additional variable δ is introduced to identify the evolution of the damage phenomena. Therefore, the kinematic variables defining the damage constitutive model are the strain $\boldsymbol{\varepsilon}$ and the internal variable $\boldsymbol{\alpha}$, which groups **D** and δ:

$$\boldsymbol{\varepsilon} \in \mathcal{D} \quad \text{and} \quad \boldsymbol{\alpha} = (\mathbf{D}, \delta) \in \mathcal{X}_1 \times \mathfrak{R} = \mathcal{X} \tag{5}$$

The thermodynamic forces conjugate to the kinematic variables are the stress $\boldsymbol{\sigma}$ and the static internal variable $\boldsymbol{\chi}$ associated with the kinematic internal variable α:

$$\boldsymbol{\sigma} \in \mathcal{S} \quad \text{and} \quad \boldsymbol{\chi} = (\mathbf{Y}, \gamma) \in \mathcal{X}_1' \times \mathfrak{R} = \mathcal{X}' \tag{6}$$

where **Y** is a second-order symmetric tensor belonging to the linear space $\mathcal{X}_1'$, and γ is a scalar variable, respectively. The constitutive equations relating the dual static and kinematic variables are written in terms of the Helmholtz free energy $\psi(\boldsymbol{\varepsilon},\mathbf{D},\delta) = \varphi(\boldsymbol{\varepsilon},\mathbf{D}) + \pi(\delta)$, which is convex in the elastic strain and in the kinematic internal variables. The functional φ: $\mathcal{D} \times \mathcal{X}_1 \rightarrow \overline{\Re}$ is convex in $\boldsymbol{\varepsilon}$ and $\mathbf{D}$, and π: $\Re \rightarrow \{+\infty\} \cup \Re$ is convex in δ. The functional φ is related to the elastic deformation but is affected by damage, while the functional π is related exclusively to damage evolution. The convex functional ψ reduces to the convex elastic energy φ in the case of non-damaging materials as

$$\varphi(\boldsymbol{\varepsilon},\mathbf{D}) = \frac{1}{2}\mathbf{E}\cdot\boldsymbol{\varepsilon}\cdot\boldsymbol{\varepsilon} \tag{7}$$

As far as the potential π is concerned, it is assumed to be a function of the kinematic damage variable δ as follows:

$$\pi(\delta) = -c_1\left[\delta + c_2 \exp\frac{\delta}{c_2}\right] \tag{8}$$

c_1 and c_2 are two material constants whose meaning will be clear later on. This is the simplest equation, with the minimum number of adjustable parameters, that still captures the experimentally observed behavior and satisfies the convexity requirement [see Equation (39)]. Hence, the constitutive equations relating the dual static and kinematic variables are written as

$$\begin{aligned}
\boldsymbol{\sigma} &= d_{\varepsilon}\psi(\boldsymbol{\varepsilon},\mathbf{D},\delta) = d_{\varepsilon}\varphi(\boldsymbol{\varepsilon},\mathbf{D}) = \mathbf{E}\cdot\boldsymbol{\varepsilon}\\
\mathbf{Y} &= -d_{\mathbf{D}}\psi(\boldsymbol{\varepsilon},\mathbf{D},\delta) = -d_{\mathbf{D}}\varphi(\boldsymbol{\varepsilon},\mathbf{D}) = -\frac{1}{2}d_{\mathbf{D}}(\mathbf{E}\cdot\boldsymbol{\varepsilon}\cdot\boldsymbol{\varepsilon})\\
\gamma &= -d_{\delta}\psi(\boldsymbol{\varepsilon},\mathbf{D},\delta) = -d_{\delta}\pi(\delta) = c_1\left[1 + \exp\frac{\delta}{c_2}\right]
\end{aligned} \tag{9}$$

where $\delta > 0$ as a result of Equation (20). The static variable **Y** is expressed as a function of the strain tensor $\boldsymbol{\varepsilon}$ in Equation (9) but it can also be written in terms of the stress tensor $\boldsymbol{\sigma}$ as well. Since the stress $\boldsymbol{\sigma}$ and the strain $\boldsymbol{\varepsilon}$ are conjugate $\varphi(\boldsymbol{\varepsilon},\mathbf{D}) = \boldsymbol{\sigma}\cdot\boldsymbol{\varepsilon} - \varphi^*(\boldsymbol{\sigma},\mathbf{D})$ and the following statement holds true:

$$\mathbf{Y} = -d_{\mathbf{D}}\varphi(\boldsymbol{\varepsilon},\mathbf{D}) = d_{\mathbf{D}}\varphi^*(\boldsymbol{\sigma},\mathbf{D}) = \frac{1}{2}d_{\mathbf{D}}(\mathbf{E}^{-1}\cdot\boldsymbol{\sigma}\cdot\boldsymbol{\sigma}) \tag{10}$$

3.2 Thermodynamic Forces

In the sequel, the lamina material directions are used as the reference frame. The damage principal directions are assumed to be coincident with the lamina material directions throughout the damage process. Then, the damage tensor **D** is characterized by its eigenvalues and can be represented as a three-component array $[\mathbf{D}] = [D_1,D_2,D_3]^T$.

Moreover, each fiber-reinforced composite lamina is characterized by a state of plane stress, but the principal directions of stress do not necessarily coincide with the damage directions. In the sequel, contracted notation [3] is used, so that the stress tensor can be represented in the damage principal frame as a three-component array $[\boldsymbol{\sigma}] = [\sigma_1,\sigma_2,\sigma_{12}]^T = [\sigma_1,\sigma_2,\sigma_6]^T$.

Then, using Equations (1) and (3), the effective stress and strain components become

$$\begin{aligned} \bar{\sigma}_1 &= \sigma_1\Omega_1^{-2} \quad ; \quad \bar{\varepsilon}_1 = \varepsilon_1\Omega_1^2 \\ \bar{\sigma}_2 &= \sigma_2\Omega_2^{-2} \quad ; \quad \bar{\varepsilon}_2 = \varepsilon_2\Omega_2^2 \\ \bar{\sigma}_6 &= \sigma_6\Omega_1^{-1}\Omega_2^{-1} \quad ; \quad \bar{\varepsilon}_6 = \varepsilon_6\Omega_1\Omega_2 \end{aligned} \tag{11}$$

Finally, the components of the static damage variable **Y** can be derived from Equation (9) as

$$\begin{aligned} Y_1 &= \frac{1}{\Omega_1^2}\left(\frac{\bar{C}_{11}}{\Omega_1^4}\sigma_1^2 + \frac{\bar{C}_{12}}{\Omega_1^2\Omega_2^2}\sigma_1\sigma_2 + \frac{\bar{C}_{66}}{\Omega_1^2\Omega_2^2}\sigma_6^2\right) \\ Y_2 &= \frac{1}{\Omega_2^2}\left(\frac{\bar{C}_{22}}{\Omega_2^4}\sigma_2^2 + \frac{\bar{C}_{12}}{\Omega_1^2\Omega_2^2}\sigma_1\sigma_2 + \frac{\bar{C}_{66}}{\Omega_1^2\Omega_2^2}\sigma_6^2\right) \\ Y_3 &= 0 \end{aligned} \tag{12}$$

where $\bar{C}_{ij}$ and Ω_i are the components of the effective elastic compliance $\bar{C} = \bar{\mathbf{E}}^{-1}$ and the integrity tensor Ω, respectively.

3.3 The Damage Domain

The irreversible damage process is modelled by assuming the existence of an admissibility domain G, called *damage domain*, in the space $\mathcal{X}'$ of the static internal variable $\chi = (\mathbf{Y},\gamma)$. The existence of the damage domain is supported by experimental evidence in the case of fibrous composites. For example, acoustic emissions associated to the nucleation of cracks and defects, were used on unidirectional fiber-reinforced composites [18,19]. It was shown that only a few acoustic pulses can be recorded during the linear portion of the stress-strain curve. Beyond the linear regime, acoustic emissions start to accelerate and are accompanied by macroscopic nonlinearity and stiffness decrease. Based on these observations, it is assumed that there exists a surface which separates the elastic domain from the damaging one. The damage criterion, which defines the current damage surface, can be expressed in terms of a damage functional $g\colon \mathcal{X}' \rightarrow \Re \cup \{+\infty\}$ and a damage-flow function $f\colon \mathcal{X}' \rightarrow \Re \cup \{+\infty\}$ such that the damage domain G can be defined as follows:

$$G = \{\chi = (\mathbf{Y}, \gamma) \in \mathcal{X}_1' \times \Re : g(\mathbf{Y}, \gamma) \leq 0\} \tag{13}$$

The surface of the damage domain can be regarded as the zero level set of the damage functional g in the space of the static internal variables, enveloping the locus of all the states which can be reached without dissipating energy through damage phenomena. The kinematic internal variable δ is related to the evolution of the damage domain during the deformation process. A uniform expansion of g, called *isotropic damage hardening,* is used in this work because (a) there is insufficient experimental evidence to justify the use of anisotropic hardening, and (b) it requires the least number of parameters and consequently the least experimental effort. Introducing the damage multiplier μ, and assuming that the damage growth is stable [10] yields

$$\dot{\boldsymbol{\alpha}} \in \mu \partial g(\chi) \tag{14}$$

with the complementary conditions

$$\mu \geq 0 \qquad g(\chi) \leq 0 \qquad \mu g(\chi) = 0 \tag{15}$$

If the static damage variable χ belongs to the interior of the damage domain G, no damage takes place, the damage multiplier μ turns out to be zero and the rate $\dot{\boldsymbol{\alpha}}$ is zero too. On the other hand, if the static damage variable χ is on the frontier of the damage domain G, then $g(\chi) = 0$, the damage multiplier can be non-vanishing and damage phenomena can occur.

The vector $\dot{\boldsymbol{\alpha}}$ has the direction of an element of sub-differential ∂f of the damage-flow function. If the function f is differentiable at the point χ on the frontier, then the sub-differential coincides with the gradient and the direction of $\dot{\boldsymbol{\alpha}}$ is uniquely defined.

In order to completely define the constitutive model, the expression of the damage functional g and the convex damage-flow f need to be specified. The following expressions are proposed here:

$$g(\chi) = g(\mathbf{Y}, \gamma) = \sqrt{\mathbf{Y} : \mathbf{J} : \mathbf{Y}} + \sqrt{|\mathbf{H} : \mathbf{Y}|} - (\gamma + \gamma_o)$$
$$f(\chi) = f(\mathbf{Y}, \gamma) = \sqrt{\mathbf{Y} : \mathbf{J} : \mathbf{Y}} - (\gamma + \gamma_o) \tag{16}$$

with γ_o being a material constant representing the initial damage threshold, **J** is a fourth-order symmetric tensor and **H** is a second-order symmetric tensor; their components being material parameters to be determined from experimental data. The damage characteristic tensors **J** and **H** can be thought of simply as material constants that define the damage surface. Determination of numerical values for these material constants from experimental data is a separate task, called model identification, which is described in detail in the next section (Section 4).

The static damage variable **Y** can be expressed in terms of the stress tensor $\boldsymbol{\sigma}$ and the damaged elastic compliance $\mathbf{E}^{-1}$, as shown in Equation (9). Particularly, each component of the static damage variable is a quadratic function of the stress components. Then, by substitution into Equation (16), the damage functional g can be given as the sum of linear and quadratic terms in the stress components in the form

$$g(\chi) = \tilde{g}(\boldsymbol{\sigma}) = \tilde{f}_{ij}\sigma_i\sigma_j + \tilde{f}_i\sigma_i .- (\gamma + \gamma_o) \qquad i, j = 1, \ldots, 6 \tag{17}$$

where $\tilde{f}_{ij}$ and $\tilde{f}_i$ are a function of both the damaged compliance tensor and the damage characteristic tensors. Hence, the proposed damage function reduces to the expression of the well known Tsai-Wu failure criterion

$$f_{ij}\sigma_i\sigma_j + f_i\sigma_i - 1 = 0 \qquad i, j = 1, \ldots, 6 \tag{18}$$

which is commonly used to predict failure of fiber-reinforced laminae in terms of experimental values of material strength [3]. The linear terms in the stress components derive from the term $\sqrt{|\mathbf{H} : \mathbf{Y}|}$. These terms play a very important role since they allow us to take into account the different behavior of PMC laminae in tension and compression. The damage threshold value γ_o and the hardening at failure γ^* are set so that $\gamma^* + \gamma_o = 1$ at failure, thus satisfying the Tsai-Wu criterion at failure.

In summary, the damage surface $g(\chi)$ in Equation (16) has the shape of a Tsai-Wu surface, which is known to represent composite material failure very well. The damage-flow $f(\chi)$ just retains the convex part of $g(\chi)$. By using a damage surface that resembles the Tsai-Wu surface, many of the observed features are brought into the model, including (a) different damage rate and threshold in tension and compression, (b) directional dependent damage rate and threshold, and (c) coupling among the various components of stress and thermodynamic forces Y.

Note that it is not postulated here that the damage model predicts failure; it only predicts damage evolution and its effect on stiffness and consequent stress redistribution. A macrocrack could precipitate failure before the critical damage D^{cr} is reached in some cases. For example, the 90-deg layer in a [0/90/0] laminate loaded in the 0-direction may fail with $D_2 < D_2^{cr}$ especially if several layers with the same orientation are clustered together. However, the 0-deg layers will sustain damage until $D_1 \cong D_1^{cr}$ [14]. Therefore, the model proposed cannot predict a macrocrack in the 90-deg layer but it can predict failure in the 0-deg layer. However, it is worth mentioning that layer clustering, where macrocracks occur, is systematically avoided in practice. Consequently, in practical laminates, distributed damage is observed nearly up to failure.

Finally, the evolutive constitutive model for damage in fiber-reinforced laminae can be finally written by assembling the constitutive Equations (9) plus the following specialized form of the evolution law (14):

$$\dot{\mathbf{D}} = \mu d_{\mathbf{Y}} f = \mu \left(\frac{\mathbf{J} : \mathbf{Y}}{\sqrt{\mathbf{Y} : \mathbf{J} : \mathbf{Y}}} \right) \tag{19}$$

$$\dot{\delta} = \mu d_{\gamma} g = -\mu \tag{20}$$

with the complementary conditions (15) and the expression (16) for the damage functional g and damage-flow f.

4. MODEL IDENTIFICATION

The constitutive model introduced in the foregoing discussion implies a number of material parameters. In all, the initial elastic properties, the damage characteristic tensors **J** and **H**, the damage threshold γ_o, and the hardening parameters c_1 and c_2 need to be determined for a single fiber-reinforced PMC lamina.

4.1 The Damage Characteristic Tensors

The damage characteristic tensors **J** and **H** define the damage domain, and together with the hardening law, define the initiation, evolution, and ultimately the fracture of the material. Therefore, the damage domain should resemble well-established failure criteria for composites, such as the Tsai-Wu failure criterion, which has been validated extensively with experimental data [3]. Although several formulations for the damage characteristic tensor **J** exist in the literature [5,21], a new form for the tensor **J** is proposed here along with the novel damage characteristic tensor **H** so that the damage domain is similar to the Tsai-Wu failure surface. In addition, the formulation results are simple enough to allow us to perform the parameter identification directly from available lamina strength data.

The principal directions of the damage characteristic tensors are supposed to be coincident with the damage principal directions. Therefore, they can be represented in matrix form as

$$[\mathbf{J}] = \begin{bmatrix} J_{11} & 0 & 0 \\ 0 & J_{22} & 0 \\ 0 & 0 & J_{33} \end{bmatrix} \qquad [\mathbf{H}] = [H_1, H_2, H_3]^T \tag{21}$$

Then, the damage functional g and damage-flow f [Equation (16)] become

$$g(\mathbf{Y},\gamma) = \sqrt{J_{11}Y_1^2 + J_{22}Y_2^2 + J_{33}Y_3^2} + \sqrt{|H_1Y_1 + H_2Y_2 + H_3Y_3|} - (\gamma + \gamma_o)$$

$$f(\mathbf{Y},\gamma) = \sqrt{J_{11}Y_1^2 + J_{22}Y_2^2 + J_{33}Y_3^2} - (\gamma + \gamma_o) \tag{22}$$

In order for the damage-flow function f to be convex, the damage characteristic tensor $\mathbf{J}$ needs to be positive definite, or $J_{ii} > 0$. The components of the damage characteristic tensors are to be determined for a single fiber-reinforced lamina by substitution of Equations (12) into Equations (22). As already pointed out, the damage function g can be written as the sum of quadratic and linear terms in the stress components σ_1, σ_2 and σ_6, the former deriving from the term $\sqrt{\mathbf{Y}:\mathbf{J}:\mathbf{Y}}$ and the latter from the term $\sqrt{|\mathbf{H}:\mathbf{Y}|}$. Then, a general procedure allows us to write the damage function, Equation (22), for different simple states of stress: tension and compression in the fiber direction, tension in the transverse direction, and inplane shear. It is then possible to derive the damage characteristic tensors in terms of the failure strengths of the material, which are known from available experimental data.

4.1.1 LONGITUDINAL UNIAXIAL LOAD

Let us consider a composite lamina subject to uniaxial load in the fiber direction. The only stress component different from zero is σ_1, and using Section 3.2, Equation (22) becomes

$$g = \sqrt{J_{11}} \frac{\bar{C}_{11}}{\Omega_1^6} \sigma_1^2 + \sqrt{|H_1| \frac{\bar{C}_{11}}{\Omega_1^6} \sigma_1} - (\gamma + \gamma_o) = 0 \tag{23}$$

The previous equation has to be satisfied from the onset of damage up to final failure of the material. Thus, if F_{1t} and F_{1c} denote the tensile and compressive strength of the fiber-reinforced lamina in the fiber direction, the following relations can be written as

$$\sqrt{J_{11}} \frac{\bar{C}_{11}}{\Omega_{1t}^6} F_{1t}^2 + \sqrt{|H_1| \frac{\bar{C}_{11}}{\Omega_{1t}^6} F_{1t}} = (\gamma^* + \gamma_o) = 1$$

$$\sqrt{J_{11}}\,\frac{\bar{C}_{11}}{\Omega_{1c}^{6}}F_{1c}^{2} + \sqrt{|H_{1}|\,\frac{\bar{C}_{11}}{\Omega_{1c}^{6}}F_{1c}} = (\gamma^{*} + \gamma_{o}) = 1 \tag{24}$$

The parameters Ω_{1t} and Ω_{1c} are the critical values of the integrity component Ω_1 for longitudinal tensile and compressive loading conditions, respectively (Section 5). In Equations (24), the term γ^* is representative of the value of the static hardening variable γ at failure. The right-hand side of Equations (24) can be compared with the right-hand side of the analogous equations written for the Tsai-Wu failure criterion:

$$\begin{aligned} f_1F_{1t} + f_{11}F_{1t}^2 &= 1 \\ f_1F_{1c} + f_{11}F_{1c}^2 &= 1 \end{aligned} \tag{25}$$

indicating that $(\gamma^* + \gamma_o) = 1$. Therefore, Equations (24) can be solved for the components J_{11} and H_1. They will turn out to be functions of the failure strength F_{1t}, F_{1c} and of the critical values of the integrity Ω_{1t}, Ω_{1c} given in Section 5.

4.1.2 TRANSVERSE UNIAXIAL LOAD

Let the fiber-reinforced lamina be subject to a transverse uniaxial load, so that the only stress component different from zero is σ_2. The expression of the damage surface (22) can be written as

$$g = \sqrt{J_{22}}\,\frac{\bar{C}_{22}}{\Omega_{2}^{6}}\sigma_{2}^{2} + \sqrt{|H_{2}|\,\frac{\bar{C}_{22}}{\Omega_{2}^{6}}\sigma_{2}} - (\gamma + \gamma_{o}) = 0 \tag{26}$$

As in the previous case, if F_{2t} is the tensile failure strength of the material in the transverse direction, then

$$\sqrt{J_{22}}\,\frac{\bar{C}_{22}}{\Omega_{2t}^{6}}F_{2t}^{2} + \sqrt{|H_{2}|\,\frac{\bar{C}_{22}}{\Omega_{2t}^{6}}F_{2t}} = (\gamma^{*} + \gamma_{o}) = 1 \tag{27}$$

where the parameter Ω_{2t} is the critical value of the integrity component Ω_2 for tensile loading in the transverse direction (Section 5). Using Equation (27), the components J_{22} can be derived as a function of H_2 as

$$J_{22} = \left(1 - \sqrt{|H_{2}|\,\frac{\bar{C}_{22}}{\Omega_{2t}^{6}}F_{2t}}\right)^{2}\left(\frac{\bar{C}_{22}}{\Omega_{2t}^{6}}F_{2t}^{2}\right)^{-2} \tag{28}$$

The behavior of a fiber-reinforced lamina will not be examined for transverse compressive loading because the critical value Ω_{2c} of the integrity component Ω_2 would have to be known and no accurate model for its evaluation is available yet. If Equation (26) could be used for the compressive failure strength F_{2c} in the transverse direction, the components J_{22} and H_2 could be determined in a closed form, as for J_{11} and H_1. As will be shown in the sequel, the component H_2 must be related to the component H_1 in order for the damage criterion to accurately describe the shear behavior of a fiber-reinforced lamina in material directions.

4.1.3 INPLANE SHEAR LOAD

Let us consider the fiber-reinforced lamina subject to a state of inplane shear, so that the only stress component different from zero is σ_6. In this case Equation (22) reduces to

$$g = \sqrt{\frac{J_{11}}{\Omega_1^4} + \frac{J_{22}}{\Omega_2^4}\frac{2\bar{C}_{66}}{\Omega_1^2\Omega_2^2}\sigma_6^2} + \sqrt{\left|\frac{H_1}{\Omega_1^2} + \frac{H_2}{\Omega_2^2}\right|\frac{2\bar{C}_{66}}{\Omega_1^2\Omega_2^2}\sigma_6} - (\gamma + \gamma_o) = 0 \quad (29)$$

Similar to the previous cases, if F_6 denotes the inplane shear strength of the lamina, then

$$\sqrt{\frac{J_{11}}{\Omega_{1s}^4} + \frac{J_{22}}{\Omega_{2s}^4}\frac{2\bar{C}_{66}}{\Omega_{1s}^2\Omega_{2s}^2}F_6^2} + \sqrt{\left|\frac{H_1}{\Omega_{1s}^2} + \frac{H_2}{\Omega_{2s}^2}\right|\frac{2\bar{C}_{66}}{\Omega_{1s}^2\Omega_{2s}^2}F_6} = (\gamma^* + \gamma_o) = 1 \quad (30)$$

where Ω_{1s} and Ω_{2s} are the critical values of the integrity component Ω_1, Ω_2 for a state of inplane shear stress. As shown in Section 5, only the value of the product of Ω_{1s} and Ω_{2s} can be determined, in the form $k_s = \Omega_{1s}^2\Omega_{2s}^2$. Since the shear response of a fiber-reinforced lamina in a material direction cannot be dependent on the sign of the shear stress, the coefficient of the linear term in Equation (30) must be zero, leading to a relationship between H_1 and H_2, namely

$$\frac{H_1}{\Omega_{1s}^2} + \frac{H_2}{\Omega_{2s}^2} = 0 \quad \Rightarrow \quad H_2 = -\frac{\Omega_{2s}^2}{\Omega_{1s}^2}H_1 = -r_s H_1 \quad (31)$$

where $r_s = (\Omega_{2s}/\Omega_{1s})^2$. Then, the component H_2 can be written as a function of the parameter r_s, and the same can be done for the component J_{22} by means of Equation (28). Hence, Equation (30) becomes

$$\sqrt{\frac{J_{11}r_s}{k_s} + \frac{J_{22}}{k_s r_s}\frac{2\bar{C}_{66}}{k_s}F_6^2} = (\gamma^* + \gamma_o) = 1$$
$$k_s = \Omega_{1s}^2\Omega_{2s}^2 \quad (32)$$

With J_{11} and H_1 known from Equation (24) and J_{22} a function of r_s from Equations (28) and (31), Equation (32) can be solved to get the value of the parameter r_s, which is then used to compute J_{22} and H_2. This completes the parameter identification except for the damage threshold γ_0 and hardening parameters c_1, c_2.

5. CRITICAL DAMAGE VALUES

The magnitude of damage at failure D_i^{cr} for each mode of failure is estimated from statistical models of the failure process for each type of loading. Refined statistical models can be used to refine the numerical values of D_i^{cr} as new knowledge about the micro-structural damage process is gained. The adopted models reflect the experience of the authors and the desire for simplicity. If supported by experimental observations, more refined models could be used without introducing any change in the proposed formulation.

5.1 Critical Damage for Longitudinal Tension

If a lamina is subject to tensile stress in the fiber direction, it is reasonable to assume that the matrix carries only a small portion of the applied load and no damage is expected in the matrix during loading. The ultimate tensile strength of the composite lamina can then be accurately predicted by computing the strength of a bundle of fibers.

All the fibers are assumed to remain elastic up to failure and to have the same stiffness. If a Weibull distribution is assumed for the strength of the fibers [23] and no significant initial fiber damage is assumed, the critical damage D_{1t} for longitudinal tensile loading can be computed as the area fraction of broken fibers in the lamina [14], which turns out to be a function of the Weibull shape modulus m as

$$D_{1t} = 1 - \exp(-1/m) \tag{33}$$

5.2 Critical Damage for Longitudinal Compression

When a fiber-reinforced lamina is compressed, the predominant damage mode appears to be fiber micro-buckling [2,29]. However, the buckling load of the fibers is lower than that of the perfect system because of fiber misalignment, so much that a small amount of fiber misalignment could cause a large reduction in the buckling load. For each misalignment angle α, the composite area-fraction with buckled fibers $\omega(\alpha)$, corresponding to fibers with misalignment angle greater than α, can be taken as a measure of damage. If the fibers are assumed to have no post-buckling strength, then the applied stress is redistributed onto the remaining unbuckled fibers, which will be carrying a higher effective stress $\bar{\sigma}$. The applied stress $\sigma = \sigma(1 - \omega)$ has a maximum which corresponds to the compressive strength of the composite. Therefore, it is possible to compute the critical damage D_{1c} for longitudinal compressive loading as

$$D_{1c} = \omega(\alpha_{cr}) = 1 - \text{erf}\left(\frac{\alpha_{cr}}{\Lambda\sqrt{2}}\right) \tag{34}$$

where erf(·) is the error function, Λ the standard deviation of the actual Gaussian distribution of fiber misalignment, and α_{cr} is the critical misalignment angle at failure (Equation (23) in Reference [2]). The characteristic misalignment Λ is determined experimentally [28] and the computation of the critical damage α_{cr} does not require any additional experimental data [2].

5.3 Critical Damage for Transverse Tension

Transverse tension can be assumed to be controlled by brittle fracture of the matrix. As for the case of longitudinal tension, the brittle loose bundle model is assumed. The material is thought of as a large number of matrix links enclosing the fibers. All the links remain linearly elastic until rupture and have the same stiffness but random stress values. A simple flat distribution can be assumed for the probability of matrix-link failure $p_f = 1/\sigma_o$, where σ_o is the strength of the strongest matrix-link. In other words, the matrix-links have random values of strength and no link is stronger than σ_o. Again, the area fraction of broken links represents the degree of damage of the lamina and the relevant effective stress can be computed. The applied stress has a maximum which corresponds to the transverse tensile strength of the fiber-reinforced lamina. As can be easily derived, the maximum stress in the bundle of matrix links turns out to be $\sigma_c = \sigma_o/4$ so that the percentage of links which are broken prior to failure is $D_{2t} = 0.5$. This model was used in Reference [11] and then applied with remarkable success in predicting the deformation and rupture of concrete specimens [12].

5.4 Critical Damage for Inplane Shear

Experimental evidence reveals a highly nonlinear behavior for a fiber-reinforced lamina subject to inplane shear. The damaged shear modulus G_{12}^* at failure can be computed as $G_{12}^* = F_6\gamma_u^{-1}$, where F_6 is the failure shear strength of the lamina and γ_u is the ultimate engineering shear strain, both of which can be experimentally determined. The value of the damaged inplane shear modulus G_{12}^* can be used to derive a measure of the induced damage as follows. The shear stress-strain law can be written in two equivalent forms:

$$\sigma_6 = 2G_{12}\varepsilon_6 \quad \text{or} \quad \bar{\sigma}_6 = 2\bar{G}_{12}\bar{\varepsilon}_6 \tag{35}$$

where $\bar{\sigma}_6$ and $\bar{\varepsilon}_6$ are the effective stress and strain inplane components, respectively. By substitution of Equation (11), the previous relation becomes

$$\bar{\sigma}_6 = 2\bar{G}_{12}\Omega_1\Omega_2\varepsilon_6 = \frac{2G_{12}\varepsilon_6}{\Omega_1\Omega_2} \tag{36}$$

so that at failure

$$k_s = \Omega_{1s}^2\Omega_{2s}^2 = \frac{G_{12}^*}{\bar{G}_{12}} \tag{37}$$

where the critical value of the product ($\Omega_{1s}^2\,\Omega_{2s}^2$) has been determined in terms of the value of the damaged and undamaged inplane shear modulus (G_{12}^* and G_{12}). Thus, only the critical value of the product of the integrity parameters Ω_{1s} and Ω_{2s} can be determined. This is a consequence of the assumption that the principal directions of the second-order damage tensor **D** remains aligned with the material principal directions over the entire life of the material. Under these conditions, shear damage is interpreted as a combination of longitudinal and transverse matrix cracks, which is supported by experimental observations [4,22]. However, as experimentally observed, most of the damage is in the form of longitudinal cracks, so that the following must be satisfied.

$$D_{2s} > D_{1s}; \qquad \Omega_{2s} < \Omega_{1s} \quad \Rightarrow \quad r_s = \frac{\Omega_{2s}^2}{\Omega_{1s}^2} < 1 \tag{38}$$

6. THE HARDENING PARAMETERS

The hardening constants γ_o, c_1 and c_2 appear in the Expression (8) of the potential π from which the hardening variable γ is derived. Let us preliminarily note that the potential π is assumed to be convex in the kinematic variable δ. Therefore, its second derivative has to be positive:

$$\pi''(\delta) = -\frac{c_1}{c_2}\exp\left(\frac{\delta}{c_2}\right) > 0 \tag{39}$$

for all the values of the variable δ. For the previous relation to be fulfilled, the material parameters c_1, c_2 need to have different signs.

The actual values of the hardening parameters are derived by comparison with experimental data. Since it has been experimentally observed that the nonlinearity of the behavior of fiber-reinforced PMC laminae is particularly severe in the case of inplane shear response, damage phenomena can be assumed to be very noticeable in this case. The basic idea is to adjust the hardening parameters to predict the response of fiber-reinforced laminae subject to inplane shear stress by means of the proposed constitutive model. Therefore, the constitutive model was implemented in the case of inplane shear stress ($\sigma_1 = \sigma_2 = 0$, $\sigma_6 \neq 0$) and the model predictions were compared with experimental data.

The parameters γ_o, c_1 and c_2 are determined by fitting the experimental shear stress-strain plot. When this plot is not available, but only the undamaged inplane shear modulus G_{12} and failure inplane shear strength F_6 are known, the curve can be reconstructed using

$$\sigma_6 = F_6 \tanh\left(\frac{G_{12}}{F_6} 2\varepsilon_6\right) \tag{40}$$

which is known to represent shear experimental data very well [1,3,4]. Since experimental values of F_6 and G_{12} are available in the literature, all the parameters of the proposed damage evolution model can be completely identified from available data.

Using the experimental data of Reference [4] for unidirectional Cytec-Fiberite M30/949 carbon/epoxy, Equation (34) yields $D_{1c}^{cr} = 0.111$ and using Equation (37)

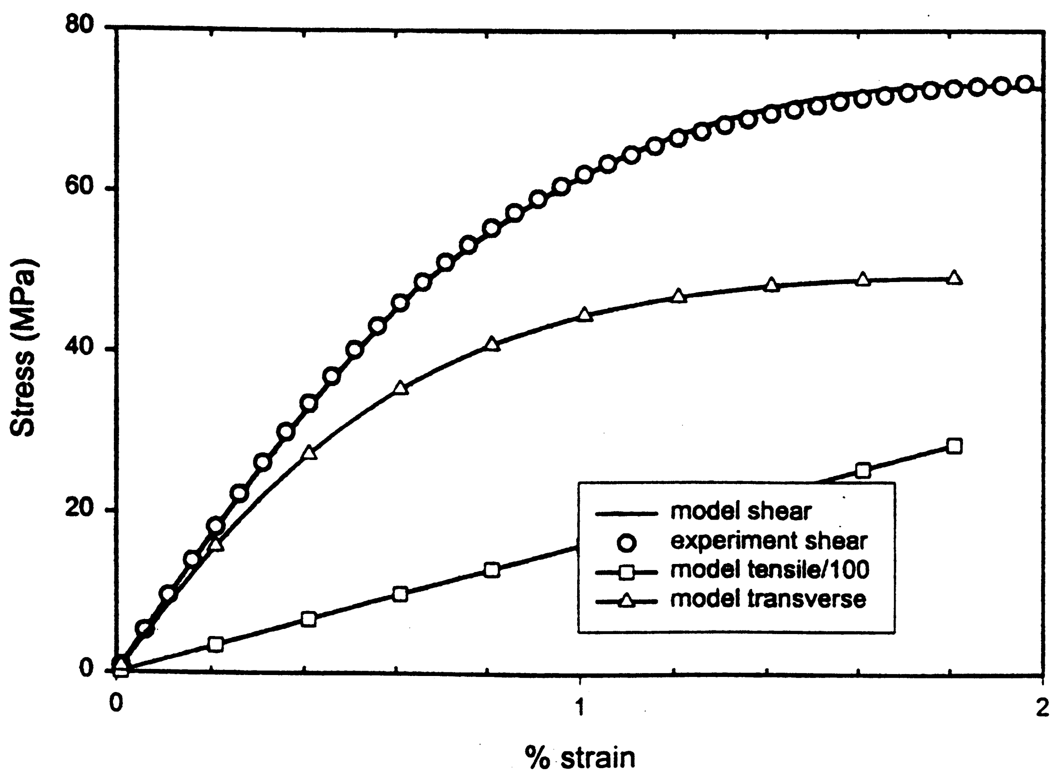

Figure 1. *Stress-strain behavior of Cytec-Fiberite M30/949 carbon/epoxy: experimental and model results.*

Table 1. Material properties and adjusted damage parameters.

Property	M30/949	M40/948	T300/5208
E_1 [GPa]	167	228	181
E_2 [GPa]	8.13	7.99	10.3
G_{12} [GPa]	4.41	4.97	7.17
υ_{12}	0.27	0.292	0.28
F_{1t} [MPa]	3060	2358	1500
F_{1c} [MPa]	1255	1462	—
F_{2t} [MPa]	35.8	43.5	52
F_6 [MPa]	75	90.3	68
k_s	0.944	0.908	0.474
D_{1t}^{cr}	0.105	0.105	0.1061
D_{1c}^{cr}	0.111	0.111	0.1109
D_{2t}^{cr}	0.5	0.5	0.500
J_{11}	0.952×10^{-15}	2.208×10^{-15}	3.147×10^{-15}
J_{22}	0.438×10^{-12}	0.214×10^{-12}	0.225×10^{-12}
H_1	25.585×10^{-9}	10.503×10^{-9}	5.303×10^{-12}
H_2	-21.665×10^{-9}	-8.130×10^{-9}	-4.712×10^{-12}
r_s	0.847	0.774	0.888
γ_0	−0.6	−0.12	−0.25
c_1	0.30	0.10	0.045
c_2	-3.95×10^5	-3.95×10^5	-4.5×10^5

$k_s = 0.944$. For carbon fibers, the measured Weibull shape modulus is $m = 9$, resulting in $D_{1t}^{cr} = 0.105$ [Equation (33)]. Finally, $D_{2t}^{cr} = 0.5$ from Section 5.3. Then, Equations (24), (27), and (32) are solved for J_{11}, J_{22}, H_1, H_2 and r_s [subject to condition (38)]. Next, the constitutive model is solved incrementally with an applied inplane shear strain and the parameters γ_0, c_1 and c_2 are adjusted to match the experimental shear stress-strain data, as shown in Figure 1. Material properties as well as damage parameters are provided in Table 1.

Then, with fixed values for the damage characteristic tensors J and H, as well as fixed values for the damage-hardening parameters γ_0, c_1, and c_2, the model is used to predict the behavior for other loading conditions. The predicted transverse stress-strain curve shows nonlinearity and the longitudinal tensile curve seems to be linear up to failure, as is routinely observed during materials testing. However, closer examination of the predicted secant stiffness, shown in Figure 2, reveals that damage takes place in all three modes of loading. A similar comparison for unidirectional Cytec-Fiberite M40/948 carbon/epoxy is shown in Figure 3.

Comparison of model and experimental shear results for unidirectional carbon/epoxy T300/5208 are shown in Figure 4, using data from Reference [9]. Then, with fixed values for J, H, γ_0, c_1, and c_2, the model is used to predict the behavior of off-axis samples. Comparison between off-axis tests and model predictions for T300/5208 with various fiber orientations are shown in Figure 5.

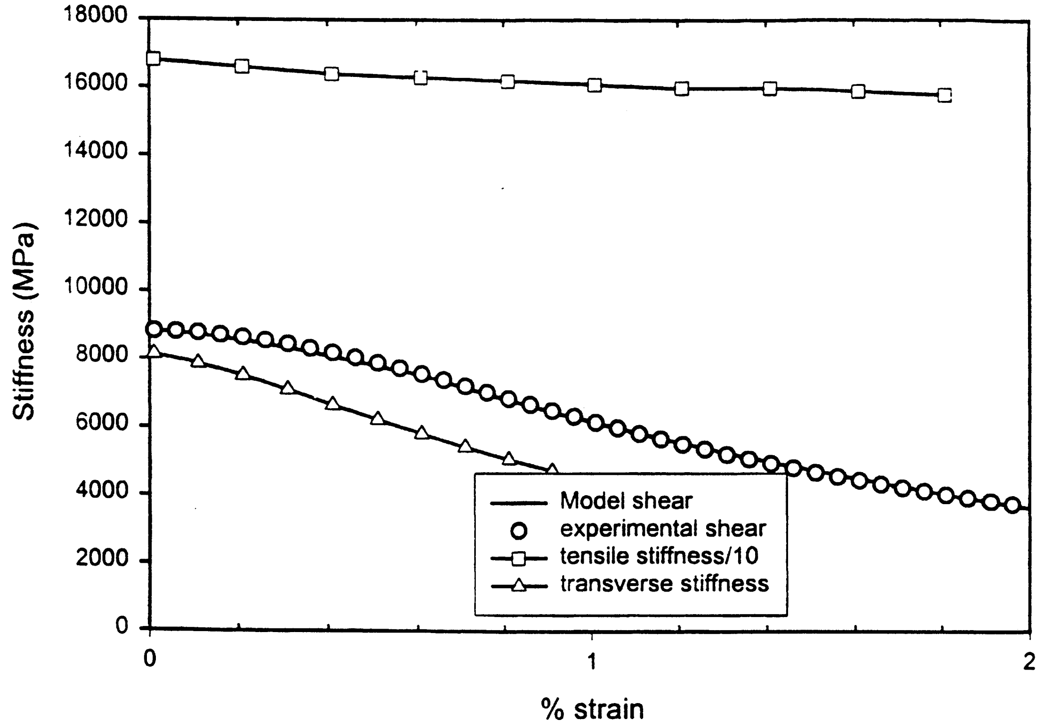

Figure 2. *Stiffness degradation of M30/949 carbon/epoxy: experimental and model results.*

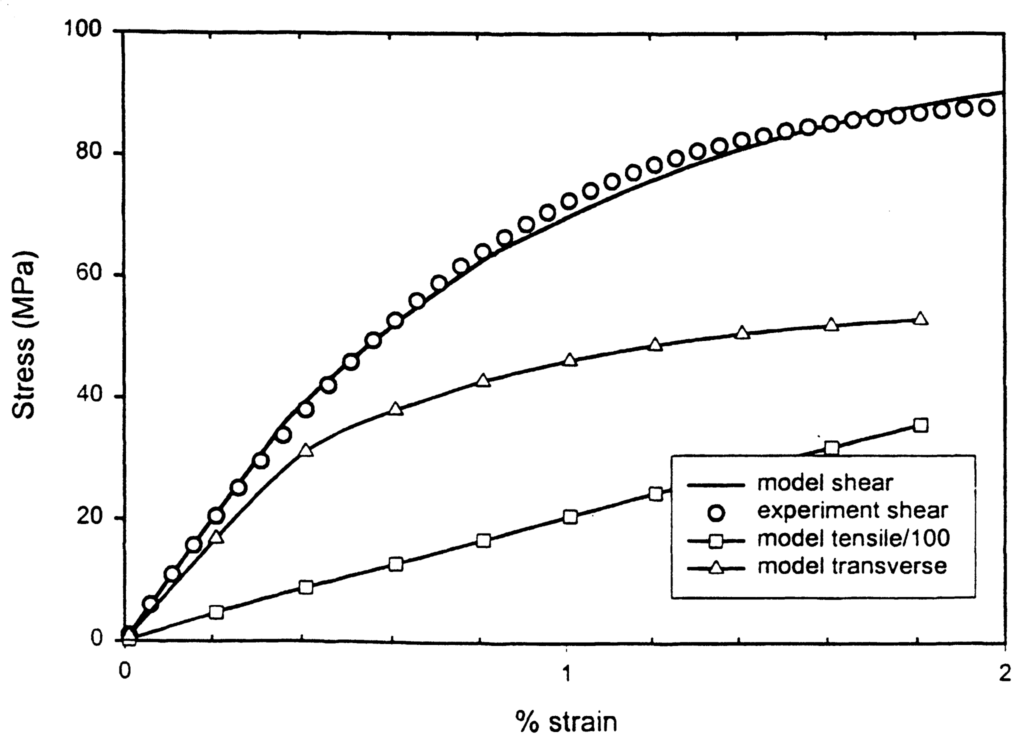

Figure 3. *Stress-strain behavior of Cytec-Fiberite M40/948 carbon/epoxy: experimental and model results.*

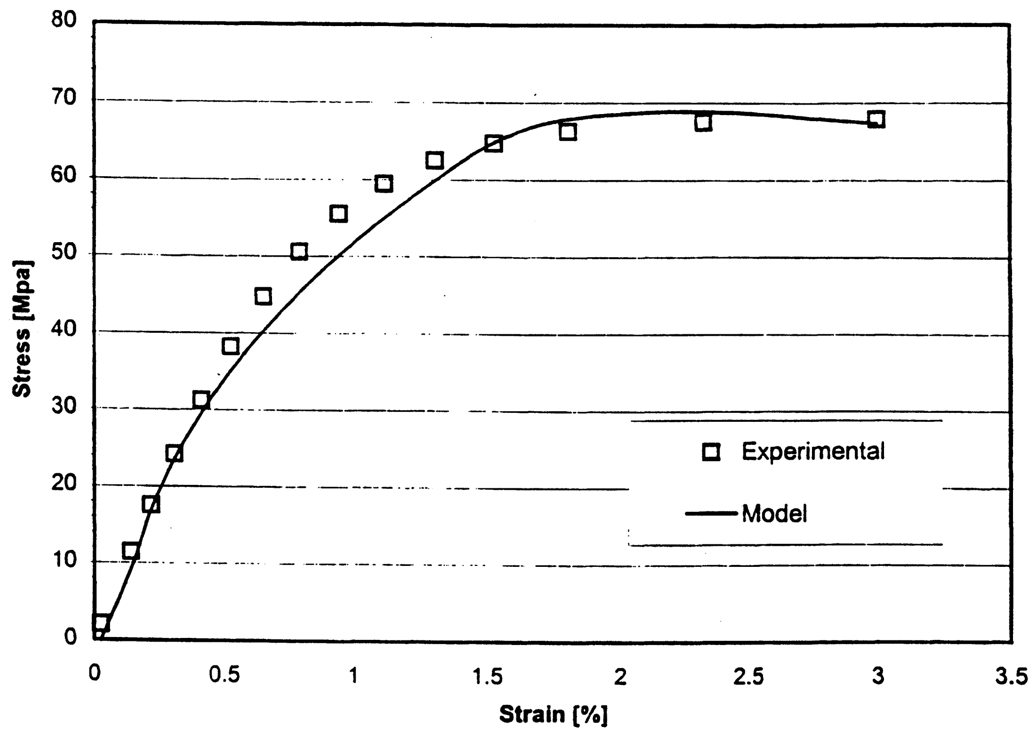

Figure 4. *Shear stress-strain behavior of T300/5208 carbon/epoxy: experimental and model results.*

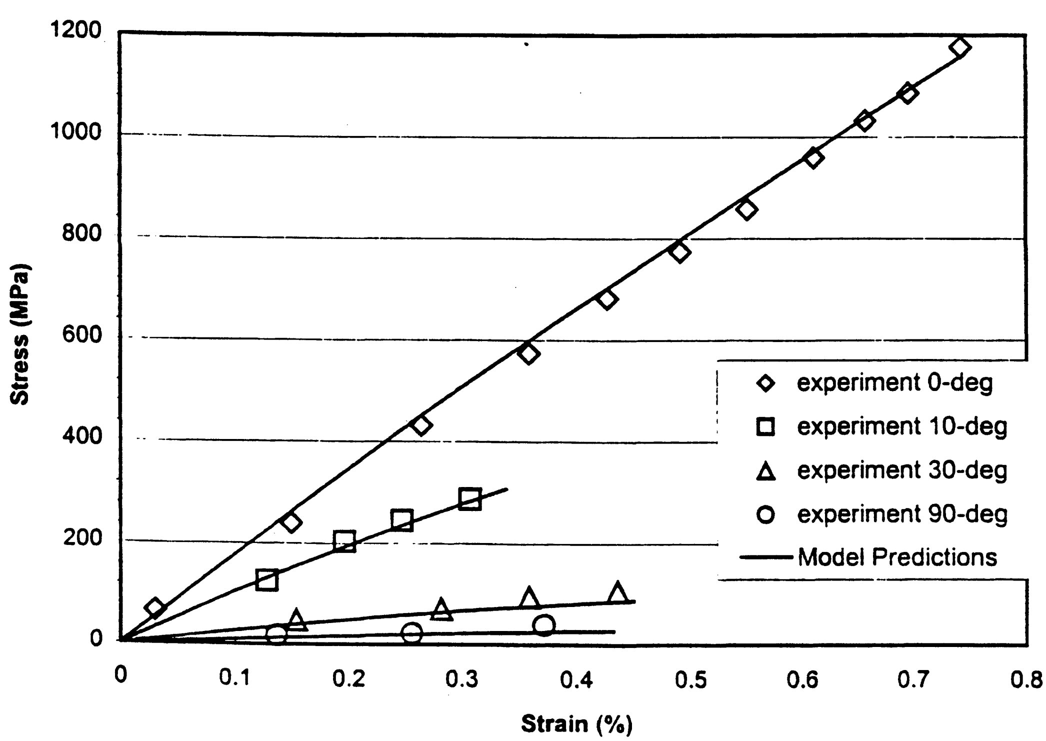

Figure 5. *Off-axis stress-strain behavior of T300/5208 carbon/epoxy: experimental and model results.*

7. CONCLUSIONS

The main advantages of the proposed model are simplicity and consistency with accepted failure criteria for composites. All parameters of the proposed model can be identified from available experimental data. The postulated damage surface reduces to the Tsai-Wu surface in stress space, thus supporting the present model with the large body of experimental evidence associated to such well known failure criteria. However, when the present model goes far beyond simple failure criteria by identifying a damage threshold, hardening parameters for the evolution of damage, and the critical values of damage for which material failure occurs. Invariance to coordinate transformation, and full interaction of stress and damage components in the thermodynamic-force space is achieved without sacrificing simplicity. Several aspects of the model allow for improvement as new experimental evidence is collected. Namely, the hardening law could be changed and the critical values of damage at failure could be refined with no change to the proposed formulation.

ACKNOWLEDGEMENT

The financial support of the National Science Foundation (USA) through grant CMS-9612162 and the Ministero della Universita a della Ricerca Scientifica (Italy) are gratefully acknowledged.

REFERENCES

1. Barbero, E. J. and J. Tomblin. 1996. "A Damage Mechanics Model for Compression Strength of Composites," *Int. J. Solids Structures*, 33(29), 4379–4393.
2. Barbero, E. J. 1998. "Prediction of Compression Strength of Unidirectional Polymer Matrix Composites," *J. Composite Materials*, 32(5), 483–502.
3. Barbero, E. J. 1999. *Introduction to Composite Materials Design*, Taylor & Francis, Philadelphia, PA.
4. Barbero, E. J. and E. A. Wen. 2000. "Compressive Strength Prediction for Production Parts without Compression Testing," ASTM STP-1383, *Composite Structures: Theory and Practice*, ASTM, PA.
5. Chow, C. L. and T. J. Lu. 1989. "On Evolution Laws of Anisotropic Damage," *Eng. Fracture Mech.*, 34(3), 679–701.
6. Cordebois, J. P. and F. Sidoroff. 1982. "Damage Induced Elastic Anisotropy," in *Mechanical Behavior of Anisotropic Solids*, J. P. Boehler, ed., Martinus Nijhoff, The Hague, 761–774.
7. Yin, W. L. 1992. "A New Theory of Kink Band Formation," AIAA-92-2552-CP.
8. Gurtin, M. E. 1981. *An Introduction to Continuum Mechanics*, Academic Press Inc., San Diego, CA.
9. Herakovich, C. T. 1998. *Mechanics of Fibrous Composites*, John Wiley, NY.
10. Ilankamban, K. and D. Krajcinovic. 1987. "A Constitutive Theory for Progressively Deteriorating Brittle Solids," *Int. J. Solids Structures*, 23(11), 1521–1534.

11. Janson, J. and J. Hult. 1977. "Damage Mechanics and Fracture Mechanics: A Combined Approach," *J. Mec. Appl.*, 1, 69–84.
12. Krajcinovic, D. 1989. "Damage Mechanics," *Mechanics of Materials*, 8, 117–197.
13. Krajcinovic, D. 1996. *Damage Mechanics*, North Holland, Amsterdam.
14. Kelly, K. and E. J. Barbero. 1993. "The Effect of Fiber Damage on the Longitudinal Creep of a CFMMC," *Int. J. Solids Structures*, 30(24), 3417–3429.
15. Liu, B. and L. B. Lessard. 1994. "Fatigue and Damage Tolerance Analysis of Composite Laminates: Stiffness Loss, Damage Modeling and Life Prediction," *Comp. Sci. Techn.*, 51, 43–51.
16. Maire, J. F. and P.-M. Lesne. 1998. "An Explicit Damage Model for the Design of Composite Structures," *Comp. Sci. Techn.*, 58, 773–778.
17. Marsden, H. 1983. *Mathematical Foundations of Elasticity*. Prentice Hall, Inc., Englewood Cliffs, NJ.
18. Liu, Y. M., T. E. Mitchell and N. G. Wadley. 1997. "Anisotropic Damage Evolution in Unidirectional Fiber Reinforced Ceramics," *Acta Materialia*, 45(10), 3981–3992.
19. Mittelman, A. and I. Roman. 1990. "Tensile Properties of Real Unidirectional Kevlar/Epoxy Composites," *Composites*, 21(1), 63–69.
20. Murakami, S. 1988. "Mechanical Modeling of Material Damage," *ASME J. Appl. Mech.*, 55, 280–286.
21. Murakami, S. and K. Kamiya. 1997. "Constitutive and Damage Evolution Equations of Elastic-Brittle Materials Based on Irreversible Thermodynamics," *Int. J. Mech. Sci.*, 39(4), 473–486.
22. Piggott, M. R., K. Liu and J. Wang. 2000. "New Experiments Suggest That All the Shear and Some Tensile Failure Processes Are Inappropriate Subjects for ASTM Standards," *ASTM STP Composite Structures: Theory and Practice*.
23. Rosen, B. W. 1964. "The Tensile Failure of Fibrous Composites," *AIAA Journal*, 2(11), 1885–1911.
24. Tong, J., F. J. Guild, S. L. Ogin and P. A. Smith. 1997. "Off-Axis Fatigue Crack Growth and the Associated Energy Release Rate in Composite Laminates," *Appl. Comp. Mat.*, 4, 349–359.
25. Voyiadjis, G. Z. and T. Park. 1995. "Anisotropic Damage of Fiber-Reinforced MMC Using Overall Damage Analysis," *J. Engng. Mech.*, 121(11), 1209–1217.
26. Voyiadjis, G. Z. and T. Park. 1995. "Local and Interfacial Damage Analysis of Metal Matrix Composites," *Int. J. Engng. Science*, 33(11), 1595–1621.
27. Voyiadjis, G. Z. and A. R. Venson. 1995. "Experimental Damage Investigation of a SiC-Ti Aluminide Metal Matrix Composite," *Int. J. Solids Structures*, 4, 338–361.
28. Yurgartis, S. W. 1987. "Measurement of Small Angle Fiber Misalignment," *Composite Science and Technology*, 30, 279–293.
29. Yurgartis, S. W. and S. S. Sternstein. 1992. "Experiments to Reveal the Role of Matrix Properties and Composite Microstructure in Longitudinal Compression Response of Composite Structures," ASTM, Nov. 16–17.